AD 263 073

TECHNICAL NOTE

D-751

INVESTIGATION OF A RETROROCKET EXHAUSTING FROM THE NOSE OF A BLUNT BODY INTO A SUPERSONIC FREE STREAM

By Nickolai Charczenko and Katherine W. Hennessey

Langley Research Center
Langley Field, Va.

NATIONAL AERONAUTICS AND SPACE ADMINISTRATION
WASHINGTON
September 1961

NATIONAL AERONAUTICS AND SPACE ADMINISTRATION

TECHNICAL NOTE D-751

INVESTIGATION OF A RETROROCKET EXHAUSTING FROM THE NOSE OF A BLUNT BODY INTO A SUPERSONIC FREE STREAM

By Nickolai Charczenko and Katherine W. Hennessey

SUMMARY

The pressure distribution and pressure drag of a blunt body with a supersonic jet issuing upstream from its center were determined at free-stream Mach numbers of 1.60, 2.00, and 2.85. The thrust of the jet issuing from the model nose was varied to study its effects on flow around the model and to determine variation of pressure distribution and pressure drag of the model with the thrust.

At all Mach numbers investigated, the pressure drag decreased with increasing retrorocket thrust until a minimum value was reached. Further increases in retrorocket thrust resulted in increases in the pressure drag. The resultant drag (pressure drag plus retrorocket thrust but excluding base and skin-friction drag) of the model was reduced by retrorocket operation below the drag for a jet-off condition, except at very low retrorocket thrust coefficients. The flow about the nose of the blunt body was very unstable throughout the range of Mach numbers and retrorocket thrust coefficients investigated.

INTRODUCTION

The safe recovery of space vehicles with little or no lift capability will depend upon an effective decelerating system. Such a system may require two or more drag devices; and drag modulation capability during a descending trajectory of a space vehicle may also be desirable. (See ref. 1.) A large number of devices for producing drag are available. Each has certain advantages and limitations and some are suitable for only certain speed ranges. In order to design a system which is most effective for a given trajectory, the aerodynamic characteristics of all these devices should be known. National Aeronautics and Space Administration is investigating a wide variety of drag devices to determine their aerodynamic characteristics and suitability for use as decelerators. (See refs. 2, 3, and 4.)

One device which has been proposed is a retrorocket. At the present time it is the only effective means of decelerating a vehicle outside the atmosphere. Its effectiveness as a decelerator or drag modulator inside the earth's atmosphere will depend on how the jet will affect the pressure and possibly skin-friction drags. This investigation was made to study the retrorocket jet effects on the pressure drag of a vehicle which has a spherical segment nose with the jet exit located in the center.

All tests were made with both angle of attack and angle of sideslip equal to 0°. They were conducted at free-stream Mach numbers of 1.60, 2.00, and 2.85 and corresponding Reynolds numbers of approximately 1.83×10^6, 1.62×10^6, and 2.14×10^6 based on the maximum frontal diameter of the model.

SYMBOLS

A	area, sq ft
C	deceleration force coefficient, $C_{d,A} + C_{d,F} + C_F$
C_D	drag coefficient, $\frac{\text{Drag}}{q_\infty A_d}$
$C_{d,A}$	afterbody pressure drag coefficient (excluding base drag), $\frac{1}{A_d} \sum_{r=2}^{r=d/2} A_i C_{p,avg}$
$C_{d,F}$	forebody pressure drag coefficient, $\frac{1}{A_d} \sum_{r=0}^{r=d/2} A_i C_{p,avg}$
C_F	thrust coefficient, $\frac{F}{q_\infty A_d}$
C_p	pressure coefficient, $\frac{p_l - p_\infty}{q_\infty}$
d	maximum body diameter

F	thrust force in drag direction due to retrorocket operation, lb
M	Mach number
p	static pressure, lb/sq ft
q	dynamic pressure, lb/sq ft
R	Reynolds number based on maximum diameter
r	local radius of model, in.
T_t	tunnel stagnation temperature, $^{\circ}F$
x	distance along model center line as indicated in figure 3, in.
α	angle of attack, deg
ϕ	meridian angle (fig. 4), deg

Subscripts:

∞	free stream
c	jet chamber
d	maximum body diameter
i	weighted
j	jet exit
l	local
avg	average

APPARATUS

Wind Tunnel

The tests were conducted in the Langley Unitary Plan wind tunnel which is a variable-pressure, return-flow tunnel. The test section is 4 by 4 feet in cross section and approximately 7 feet long. The Mach number may be varied from 1.5 to 2.9 in any desired increment without

tunnel shutdown by operating an asymmetric sliding block. Further details of the tunnel may be obtained from reference 5.

Model and Support System

A sketch of the model with the support system is shown in figure 1. The support strut contained lines for transmitting the high-pressure air used to simulate the retrorocket jet exhaust. Tubing from the pressure orifices on the model to the pressure measuring system was also led through the support strut.

The model, which is shown in greater detail in figure 2, had a conical frustum afterbody with an 8.28-inch diameter at the front and 4.0-inch diameter at the base. The forebody of the model is a spherical segment of 8.9-inch radius in the center of which is located the retrorocket nozzle exit. The nozzle has an area ratio $\left(\frac{\text{Exit area}}{\text{Throat area}}\right)$ of 4, a half angle of 26.5° and a throat diameter of 0.15 inch. The model is instrumented with 35 pressure orifices, 14 of which are located on the forebody and 21 on the conical frustum. The location of those orifices is shown in figure 3.

Air Supply for Jet Simulation

The high-pressure air used to simulate the exhaust from the retrorocket was supplied from a bottle field with a capacity of about 900 cubic feet. This air supply could provide a maximum pressure of 2,400 pounds per square inch, a sustained flow rate of 2 pounds per second or maximum flow rate of 11 pounds per second for 10 seconds.

INSTRUMENTATION AND ACCURACY

Pressure measurements on the surface of the model were made by connecting the orifices to automatic switching valves which sampled each pressure in sequence and transmitted the pressure to a single transducer. The transducer output was digitized and punched into cards for machine calculation of the pressure coefficient. A 15-pound-per-square-inch transducer was used to measure the hemispherical nose pressures, and a 5-pound-per-square-inch transducer was used for the conical-afterbody pressures to increase the accuracy of measurements on this surface. The free-stream and stagnation pressures were measured on precision mercury manometers accurate to within 0.5 pound per square foot. Chamber pressure of the retrorocket nozzle was measured by means of a 1,500-pound-per-square-inch transducer and probe (located as shown in fig. 2).

From previous calibrations, it is estimated that the accuracies of the angle of attack and angle of sideslip are within ±0.15°. The deviations due to flow angularity have been compensated by adjusting the angle of attack of the model at each Mach number. The maximum deviation of the free-stream Mach number in the range covered by these tests is ±0.02. The accuracies of the quantities, C_p and C_F which were dependent on free-stream conditions are estimated to be as follows:

M_∞	$\pm\Delta C_p$ for afterbody	$\pm\Delta C_p$ for forebody	$\pm\Delta C_F$
1.60	0.0060	0.0178	0.0131
2.00	.0070	.0209	.0155
2.85	.0065	.0194	.0143

TESTS AND REDUCTION OF DATA

With the angle of attack and angle of sideslip of the model set at zero, pressure coefficients were obtained for the following test conditions:

M	R	q_∞	T_t, °F	Maximum p_c, psi
1.60	1.83×10^6	607	125	1,040
2.00	1.62	516	125	1,150
2.85	2.14	558	150	1,140

The thrust was calculated from the chamber pressure on the assumption that the flow in the nozzle was fully expanded and the Mach number at the jet exit is that determined by the area ratio of the nozzle for a perfect gas. The equation used in calculating the thrust is:

$$F = A_j \left(2q_j + p_j - p_\infty \right)$$

$$F = A_j \left(0.3904 p_c - p_\infty \right)$$

It was further assumed that the pressure at the nozzle exit is the free-stream static pressure. This assumption is justified on the basis

that the second term in the thrust equation represents a small portion of the total thrust. The error introduced due to these assumptions is believed to be small.

The thrust coefficient was based on the free-stream dynamic pressure and maximum frontal area of the model so that the thrust and drag coefficient would be directly comparable. The values for the pressure drag were obtained by multiplying the average pressure coefficient at a given radial station by an annulus whose boundaries were located midway between orifices. These values were added to obtain the pressure drag of the model.

RESULTS AND DISCUSSION

Flow Stability

The supersonic air flow from the nozzle located in the center of the forebody causes a very unsteady flow in the vicinity of the model. The exact source of this instability is not known. However, there are several factors that could have contributed toward this condition. One factor to be considered is the fluctuation in pressure on the forebody, which can be self-sustained if looked upon from the following point of view. The pressure in the subsonic region adjacent to the free jet boundary depends to a large degree on the shape of the bow shock. When the bow shock has a rounded shape (essentially normal shock), the pressure behind it is large. This large static pressure adjacent to the free jet boundary limits jet expansion and forces it to assume an elongated form. The jet produces the same results as a spike protruding from the forebody into the free stream and changes the bow shock from a blunt to a conical shape. The pressure behind an oblique shock is smaller than it is behind a blunt shock; thus the pressure adjacent to the free jet boundary is reduced. The reduction in pressure allows greater expansion of the jet which causes the bow shock to become more rounded and the cycle starts over again.

Some typical variations in shock pattern are shown in figure 4. These schlieren pictures were taken in succession for identical flow conditions, one at $M = 1.60$ and the other at $M = 2.00$. In this figure one can see that the bow shock changes its shape and location from a blunt, rounded form close to the forebody to a conical form further away from the nose of the model.

Other factors that could have influenced the stability of the flow are fluctuations in chamber pressure and small lateral oscillations of the model. Since there was no dynamic record of the chamber pressure made, it cannot be stated that there was no fluctuation in the chamber pressure. Such fluctuation if it existed, would affect the outside

flow through a variation in mass flow and jet exit pressure. The model was also subject to small lateral oscillations induced by the tunnel air flow because it was supported on a long and relatively thin strut. It is believed that these two factors, even though they might have contributed to the instability of the flow, are not the primary causes of the flow instability.

This flow instability, which existed at all Mach numbers and thrust coefficients, has its greatest effect on the forebody pressures, whereas the pressures on the conical part of the body are almost unaffected. The amplitude of pressure fluctuations on the forebody is of the order of 10 percent of the average pressure level at a given orifice and the amplitude increases slightly at lower thrusts. Because of the flow instability, the average pressures were computed by adding the pressures at each radial station and dividing by the number of orifices. Average pressures are used throughout this report in pressure plots and for pressure drag computations.

Effects of Jet Exhaust on the Pressure Distribution About the Model

In figure 5, the experimental pressure distribution on the forebody is presented for various thrust coefficients at Mach numbers 1.60, 2.00, and 2.85. The pressure distribution on the forebody with the jet off is closely approximated by Newtonian theory as was shown in reference 6. In reference 6 a similar model was used to obtain pressure data at various angles of attack. The data of reference 6 for $\alpha = 0^\circ$, are compared with the present data for the jet-off condition, and as can be seen in figure 5, they are in good agreement. A small amount of air flow from the nozzle produces a large reduction in pressure on the forebody, particularly in the vicinity of jet exit, where with the jet off, there was a high stagnation pressure. This large reduction in pressure which occurs near the nozzle exit becomes smaller with increasing distance away from the nozzle. At low thrust, part of the forebody near the outer edges experiences an increase in pressure. However, with further increases in thrust, a reduction in pressure occurs over the entire forebody. This reduction in pressure on the forebody continues until a minimum is reached and the pressures on the forebody begin to increase with further increases in thrust except at $M = 1.60$ where the maximum thrust available was not sufficient to reach this condition. For a Mach number of 2.00, the maximum reduction in pressure on the forebody occurs between the thrust coefficients of 0.148 and 0.163; for a Mach number of 2.85, the maximum reduction occurs between thrust coefficients of 0.125 and 0.150.

A noticeable decrease in pressure on the forebody at a constant thrust is also observed with the increase in free-stream Mach number and indicates greater jet effects on the forebody pressures at higher Mach numbers.

In general, the variation of pressure distribution on the forebody with increasing thrust is very similar to the pressure distribution on a blunt nose with a spike attached at the center. (See ref. 7.) The reference shows that increasing the length of the spike results in a decrease of pressure on the forebody (same as increasing the thrust) until a minimum pressure is reached corresponding to a point where the origin of separation begins to change from the tip of the spike to the downstream surface.

The jet effects on the longitudinal pressure distribution on the entire model at various Mach numbers are shown in figure 6. At Mach numbers of 1.60 and 2.00 for the jet-off condition, the flow was separated over the entire surface of the conical afterbody. (See figs. 7(a) and 7(b).) The separation was most pronounced at the lowest Mach number. At all Mach numbers, the flow had to expand from a subsonic flow in front of the forebody to a supersonic flow on the afterbody. This expansion required low pressures on the afterbody and, since the afterbody pressures were too high for the full expansion of the flow at the lower Mach numbers, the flow was separated in that region. The presence of the jet changed the shape of the bow shock and thus made it similar to a detached bow shock in front of a cone. This condition resulted in a reduction and, in some instances, elimination of the separation over the afterbody. Consequently, the jet effects on the afterbody were greatest at a Mach number of 1.60 where the largest reduction in pressure was experienced.

Jet Effects on the Drag of the Model

The pressure drag of the forebody and the afterbody excluding the base is presented separately in figure 8 so that the drag contribution of each part may be seen more clearly. Inasmuch as the pressure drag of the model is directly related to the pressure distribution on the model, the jet effects on the pressure drag will closely resemble the jet effects on the pressure distribution. A variation of pressure drag of the forebody with thrust coefficient is shown in figure 8(a) for different Mach numbers. A high stagnation pressure that exists in front of the body with the jet off, which accounts for a large pressure drag contribution of the forebody, is greatly reduced by a supersonic flow from a small jet located in the center of the forebody. The pressure drag of the forebody continues to decrease with increasing thrust until a minimum pressure drag is reached, at which point the pressure

drag starts increasing with further increases in thrust. The data in figure 8 indicate that the point of minimum pressure drag occurs at lower thrust coefficients for the higher Mach numbers.

The pressure drag of the afterbody (fig. 8(b)) increases with a decrease in Mach number with the jet on. This increase in drag resulted from the change of flow on the afterbody which was previously discussed. An interesting point about the afterbody pressure drag is that, after reaching a certain level at a given Mach number, it remained almost constant with increases in thrust.

In figure 9, the contribution to the pressure drag of separate parts of the model are added together with the drag due to thrust to obtain the resultant drag of the model. It should be kept in mind that, in computing the resultant drag of the model, the pressure at the base was assumed to be the free-stream pressure and that the friction drag was not taken into consideration. However, in view of the fact that the afterbody pressures remained almost constant with increases in thrust coefficient, it is believed that the base pressures, although they will be smaller than the free-stream pressure, will not vary appreciably with increases in thrust. Thus the trend of the resultant-drag curves will not be altered significantly, but they will be shifted to a slightly higher level. Some indication of the effects of a jet exhausting into a supersonic stream on the friction drag of a body may be found in reference 8.

A summary of the results of this investigation is presented in figure 10. Here the variation of the decelerating force coefficient (pressure drag plus retrorocket thrust but exclusive of base and skin-friction drag) with thrust coefficient is shown at various Mach numbers. These results indicate that a retrorocket located in the center of a blunt body may increase drag by a small amount at very low thrust coefficient. At higher thrust coefficients, the total drag of the model is reduced far below the value of the drag with the jet off, and great amounts of thrust would be required before any drag due to the jet will be realized as the extrapolation of these curves indicates. Thus the retrorocket which could be used effectively in regions of very low density (outside of the atmosphere) or perhaps for a soft landing does not look promising for use as a decelerator at supersonic speeds in regions of relatively high density. Although some improvements in drag might be achieved by locating several nozzles on the periphery of the blunt body, the problem of flow instability most likely will still be present. The retrorocket, even though it does not look promising for use as a decelerator, may be utilized as a drag modulator where the primary interest is not in the maximum drag that can be achieved but in controlled drag.

CONCLUSIONS

An investigation of an air jet simulating a retrorocket exhausting into a supersonic free stream from the nose of a blunt body led to the following conclusions:

1. A flow instability about the nose of the blunt body occurred throughout the range of Mach numbers and retrorocket thrust coefficients investigated. The forebody pressures were affected most by this flow instability.

2. The retrorocket exhaust caused large reductions in pressure over the nose of the blunt body and these reductions in pressure become greater with increases in the free-stream Mach number.

3. A large decrease in pressure drag occurred as a result of retrorocket operation at all Mach numbers of the investigation. This pressure drag decreased with increasing retrorocket thrust until a minimum was reached. Further increases in retrorocket thrust resulted in increases in the pressure drag.

4. The resultant drag (pressure drag plus retrorocket thrust but excluding base and skin-friction drag) of the model was reduced by retrorocket operation below the drag for a jet-off condition, except at very low retrorocket thrust coefficients. The results indicate that very large retrorocket thrust coefficients would be required to produce decelerating forces much in excess of the jet-off drag forces.

Langley Research Center,
National Aeronautics and Space Administration,
Langley Field, Va., April 3, 1961.

REFERENCES

1. Phillips, Richard L., and Cohen, Clarence B.: Use of Drag Modulation To Reduce Deceleration Loads During Atmospheric Entry. ARS Jour., vol. 29, no. 6, June 1959, pp. 414-422.

2. Maynard, Julian D.: Aerodynamic Characteristics of Parachutes at Mach Numbers From 1.6 to 3. NASA TN D-752, 1961.

3. Maynard, Julian D.: Aerodynamics of Decelerators at Supersonic Speeds. Proc. of Recovery of Space Vehicles Symposium, Los Angeles, Calif., Aug. 31 - Sept. 1, 1960. (Sponsored by Inst. Aero. Sci. and Air Res. Dev. Command.)

4. McShera, John T., and Keyes, J. Wayne: Wind-Tunnel Investigation of a Balloon as a Towed Decelerator at Mach Numbers From 1.47 to 2.50. NASA TN D-919, 1961.

5. Anon.: Manual for Users of the Unitary Plan Wind Tunnel Facilities of the National Advisory Committee for Aeronautics. NACA, 1956.

6. Newlander, Robert A., Taylor, Nancy L., Pritchard, E. Brian: Pressure Distribution on Two Models of a Project Mercury Capsule for a Mach Number Range of 1.60 to 6.01 and an Angle-of-Attack Range of 0° to 180°. NASA TM X-336, 1961.

7. Moeckel, W. E.: Flow Separation Ahead of a Blunt Axially Symmetric Body at Mach Numbers 1.76 to 2.10. NACA RM E51I23, 1951.

8. Love, Eugene S.: The Effect of Small Jet of Air Exhausting From the Nose of a Body of Revolution in Supersonic Flow. NACA RM L52I19a, 1952.

L
1
5
0
4

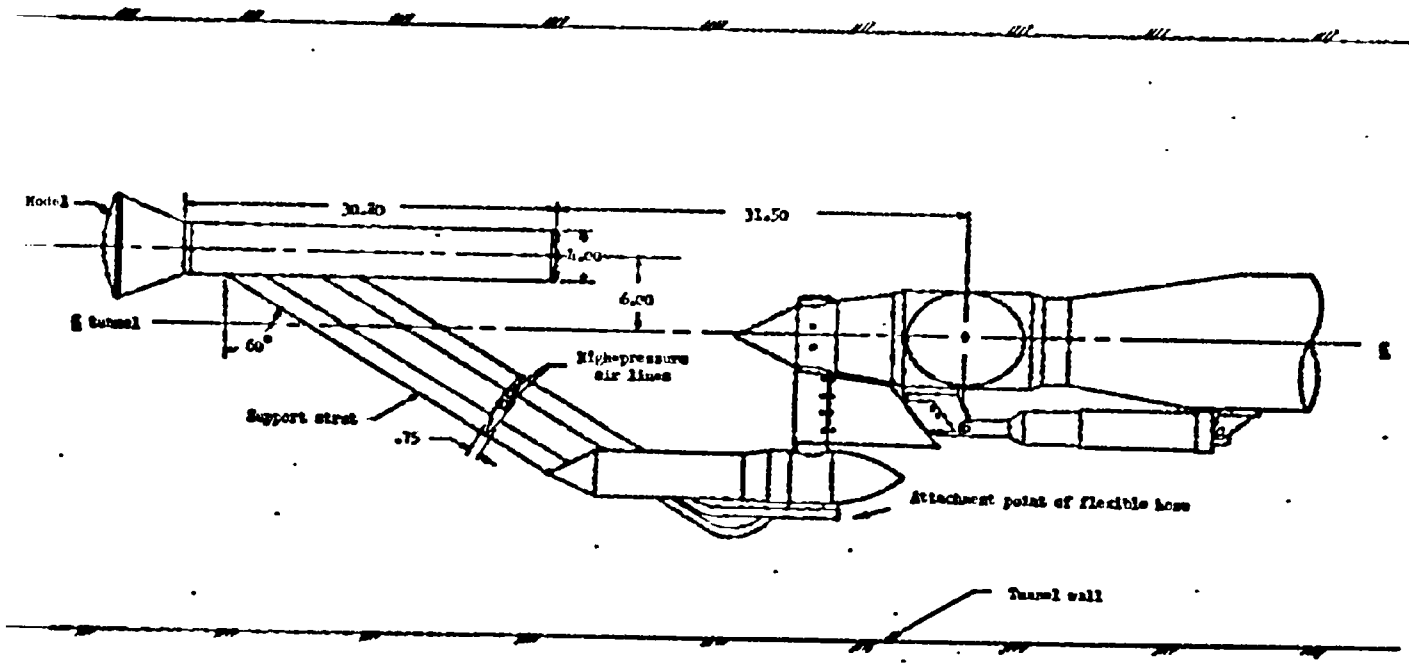

Figure 1.- Drawing of the model and model support arrangement. All dimensions are in inches.

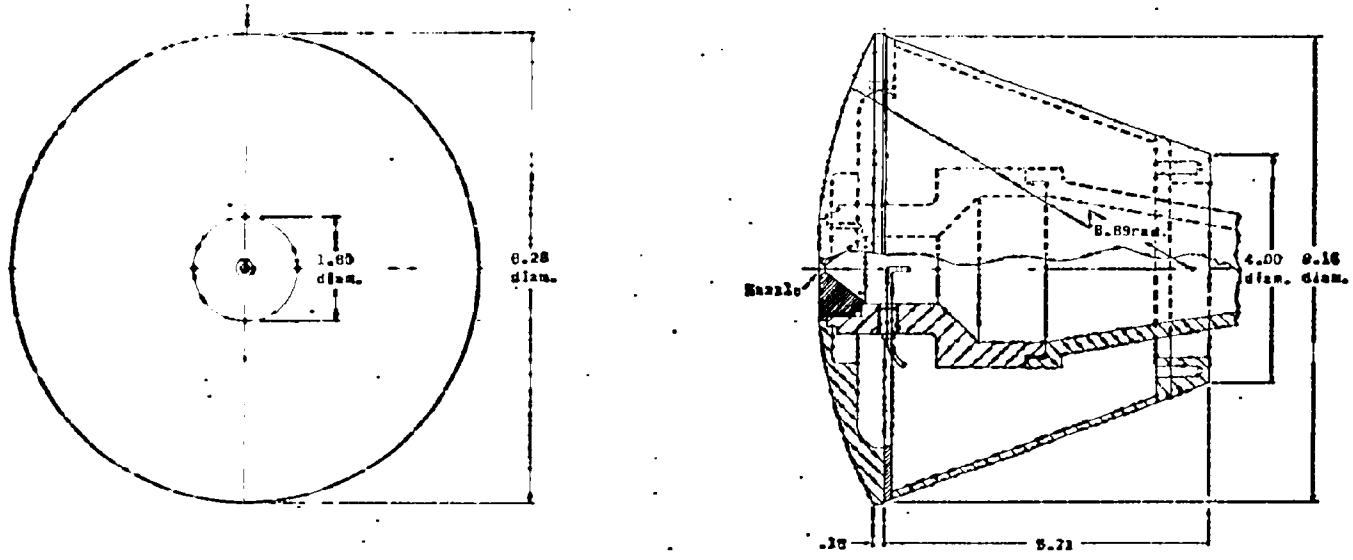

Figure 2.- Model drawing. All dimensions are in inches.

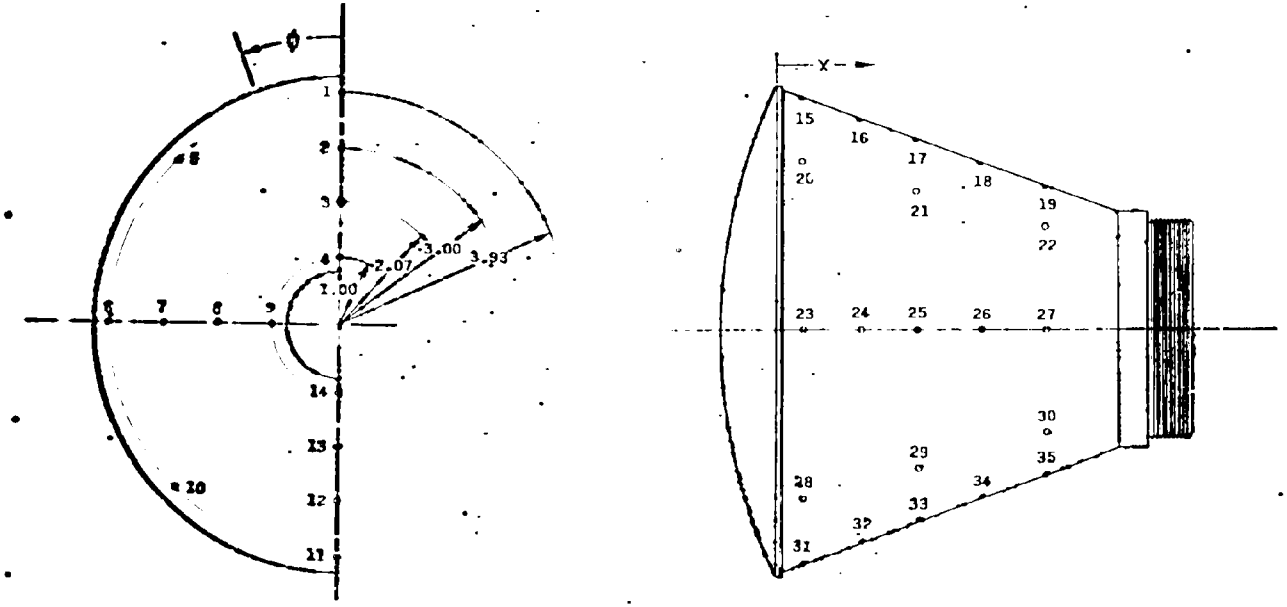

r/ro	r/ro	φ/deg 0°	45°	90°	135°	180°
-0.95	1.00	4		9		14
-0.77	2.07	3		8		13
-0.50	3.00	2		7		12
-0.09	3.93	1	5	6	10	11
0.36		15	20	23	28	31
1.33		16		24		32
2.29		17	21	25	29	33
3.40		18		26		34
4.51		19	22	27	30	35

Figure 3.- Pressure orifice location on the model.

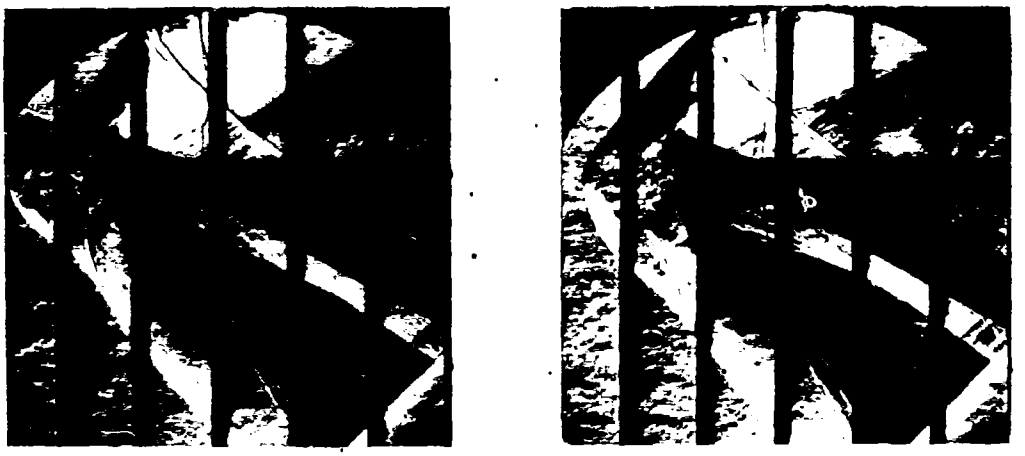

(a) $M = 1.60$; $C_T = 0.055$.

(b) $M = 2.00$; $C_T = 0.163$. L-61-1087

Figure 4.- Typical schlieren photographs of variation in shock pattern for a constant thrust coefficient.

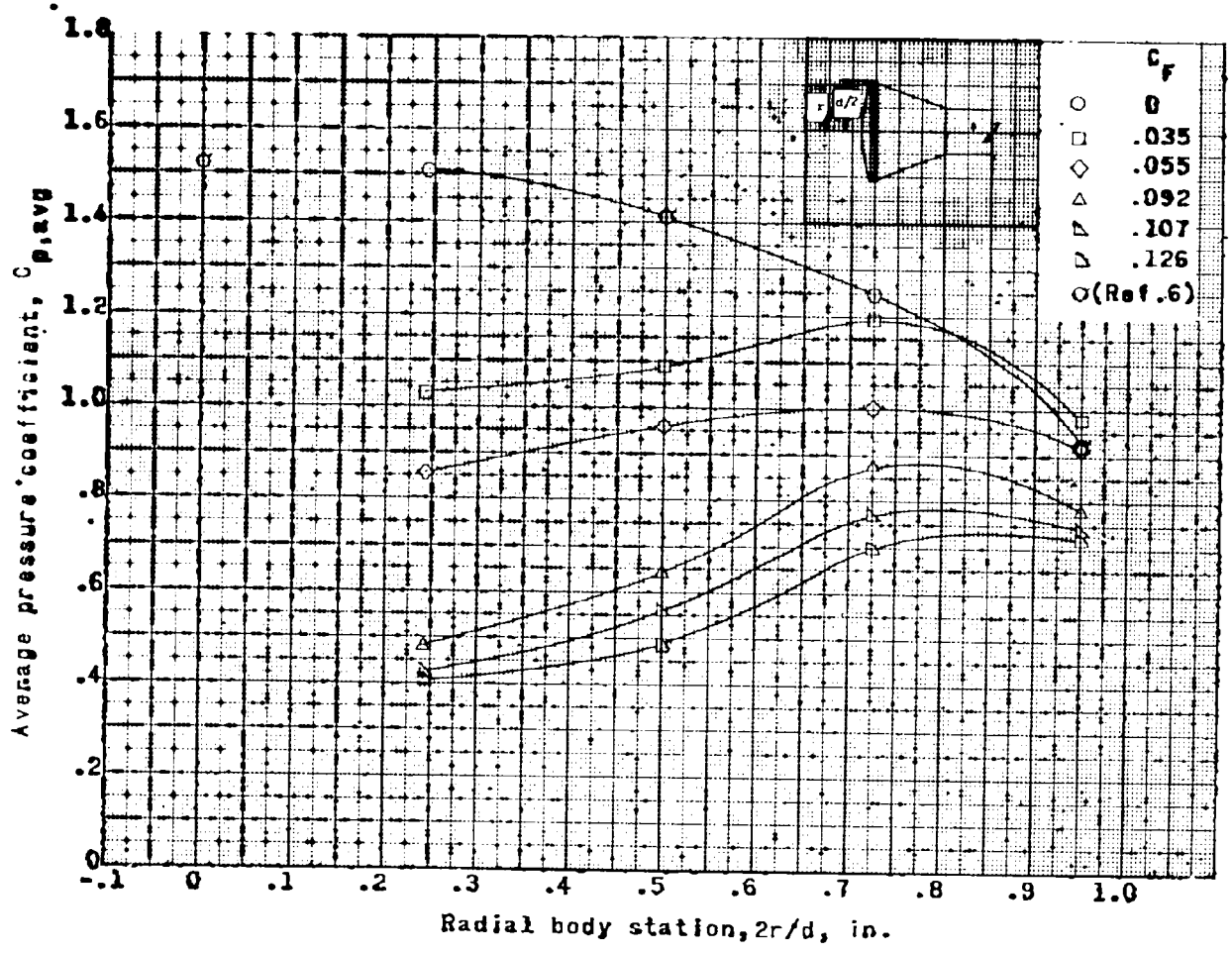

(a) M = 1.60.

Figure 5.- Effect of jet exhaust on the radial pressure distribution of the model forebody.

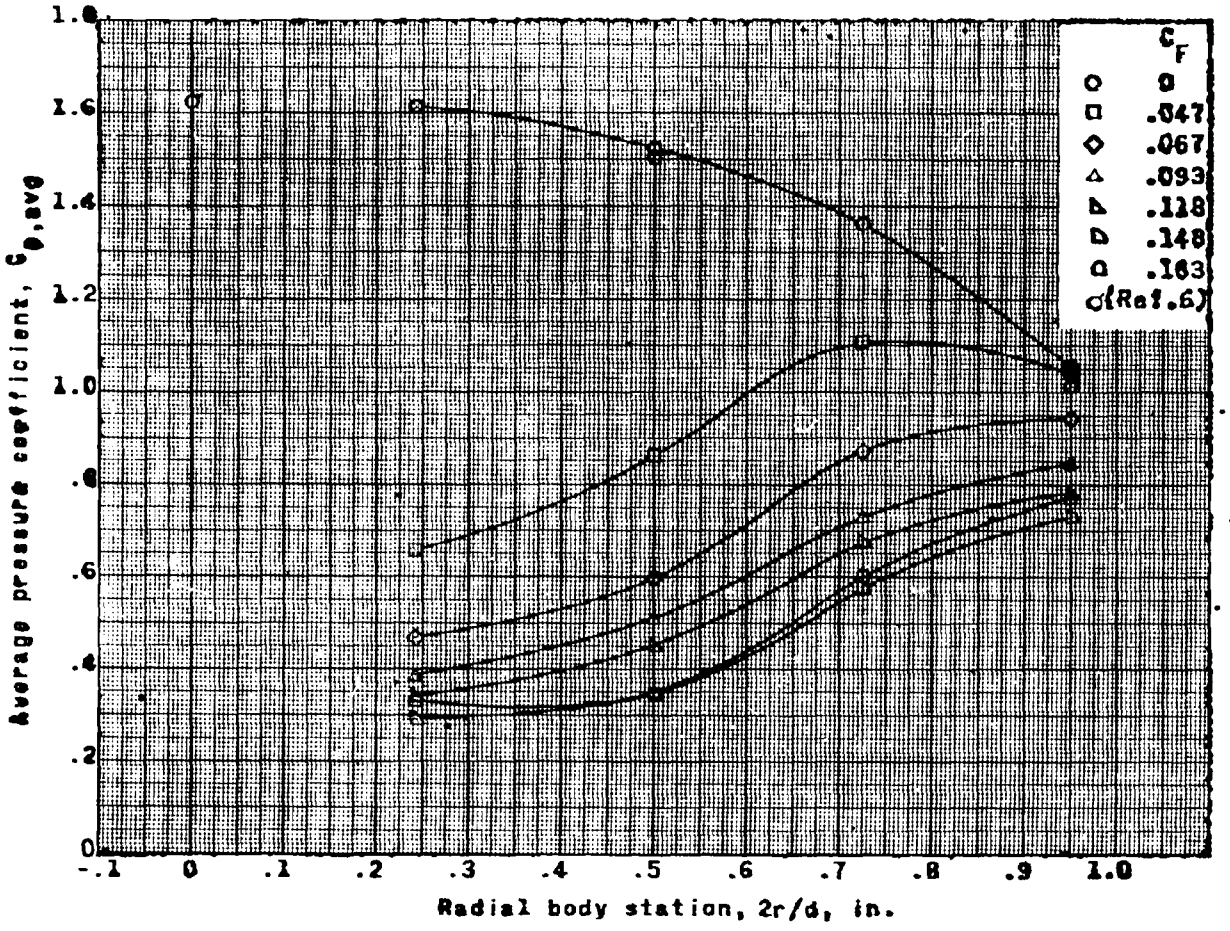

(b) M = 2.00.

Figure 5.- Continued.

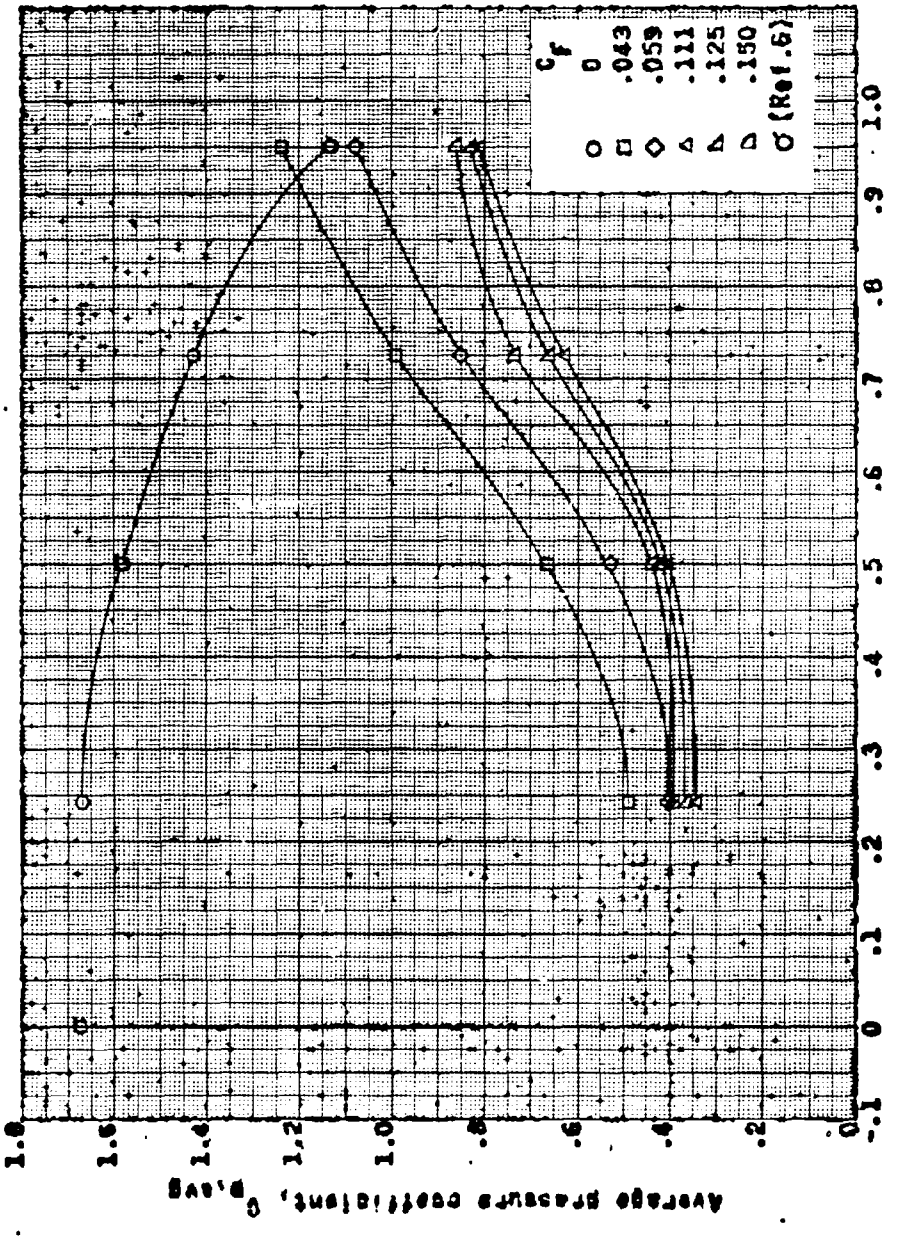

(e) M = 2.85.

Figure 5.- Concluded.

L-1504

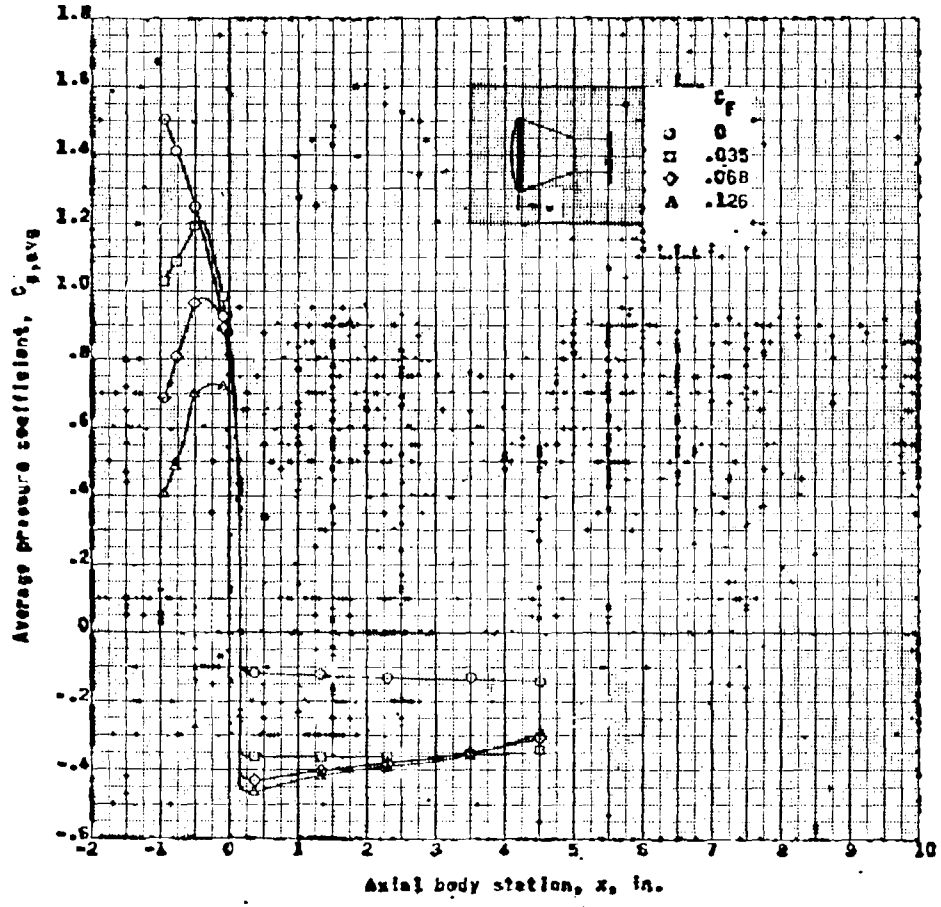

(a) M = 1.60.

Figure 6.- Effect of jet exhaust on the longitudinal pressure distribution along the entire body.

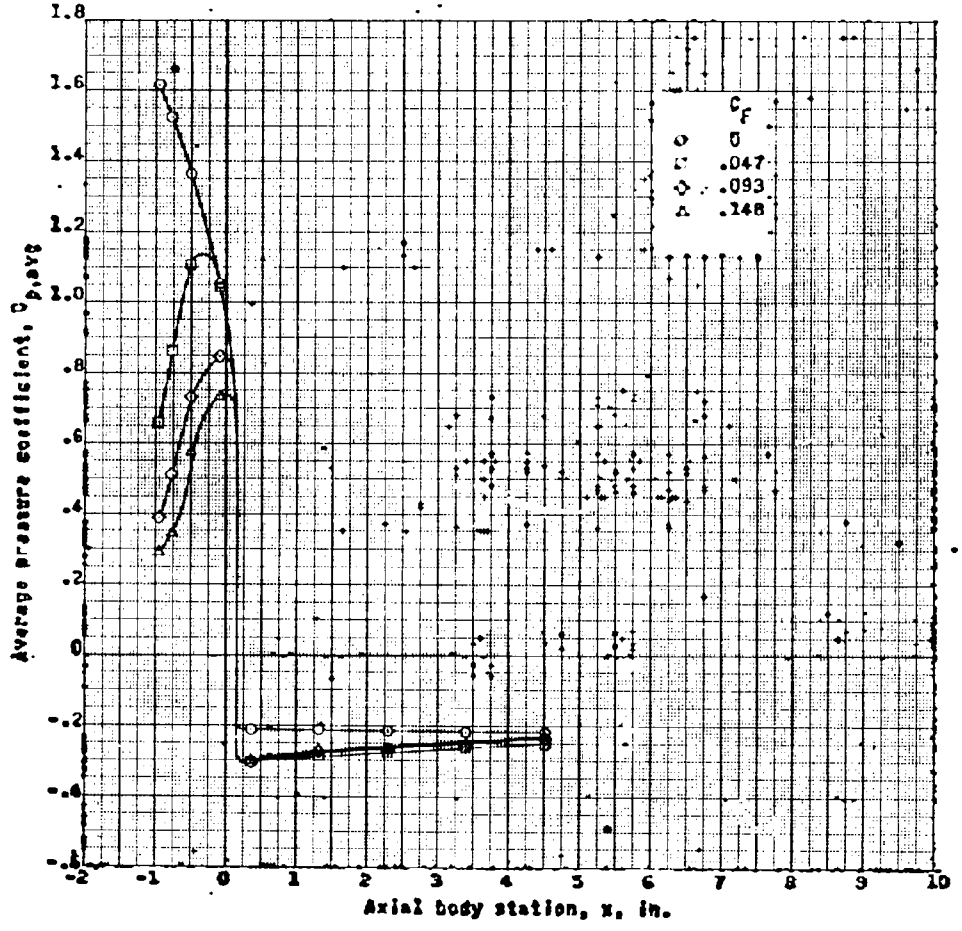

(b) M = 2.00.

Figure 6.- Continued.

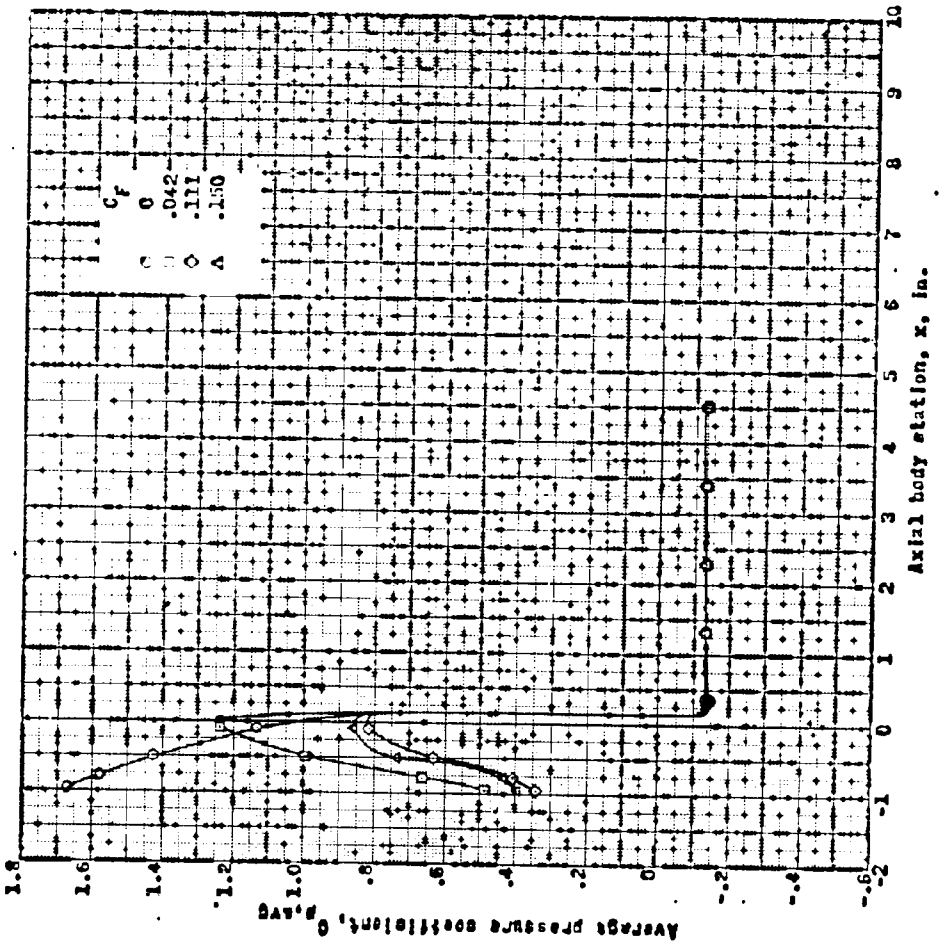

(c) $M = 2.85$.

Figure 6.- Concluded.

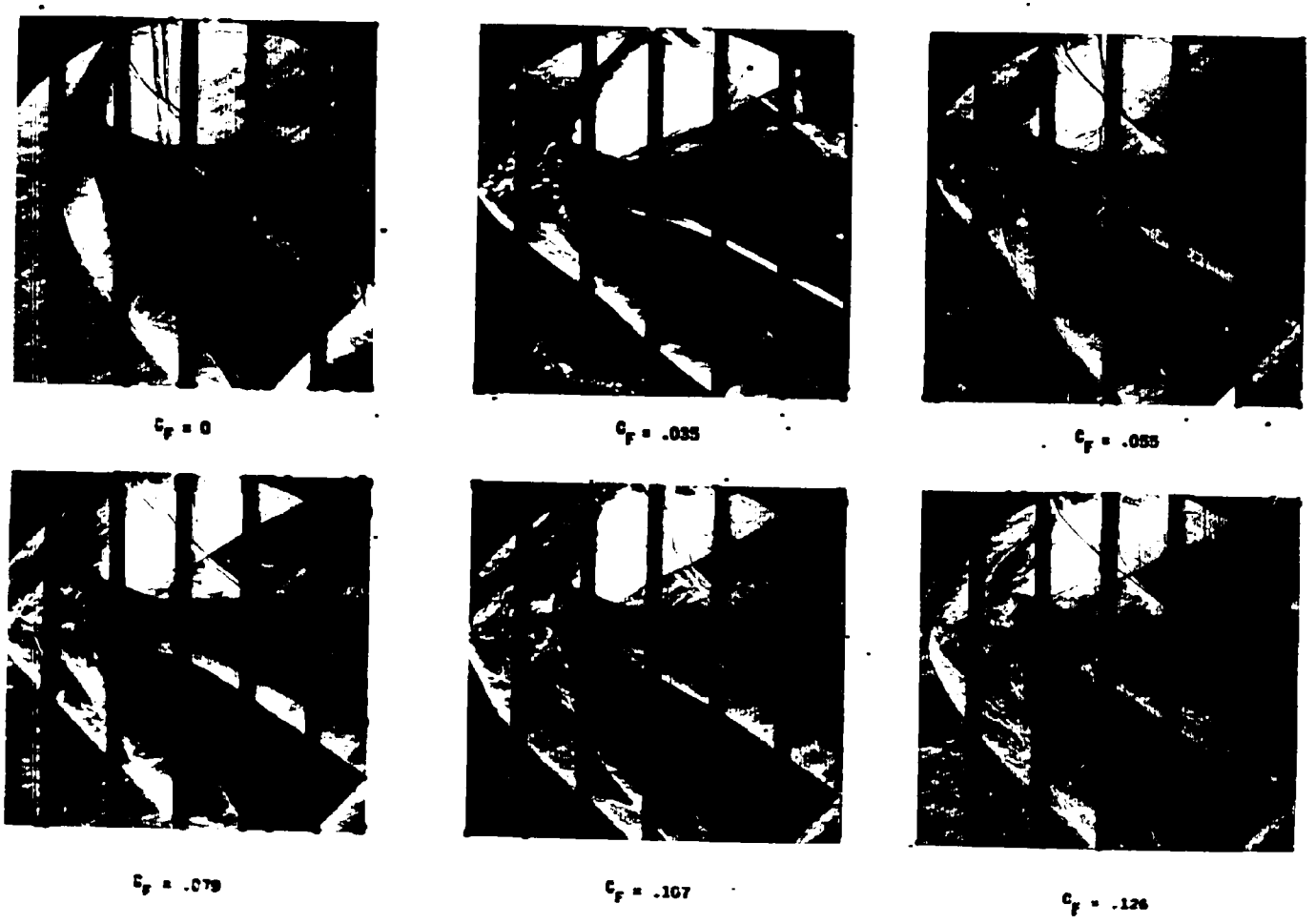

(a) M = 1.60. L-61-1088

Figure 7.- Typical schlieren photographs of the flow field about a blunt body with the jet exhausting into a supersonic stream.

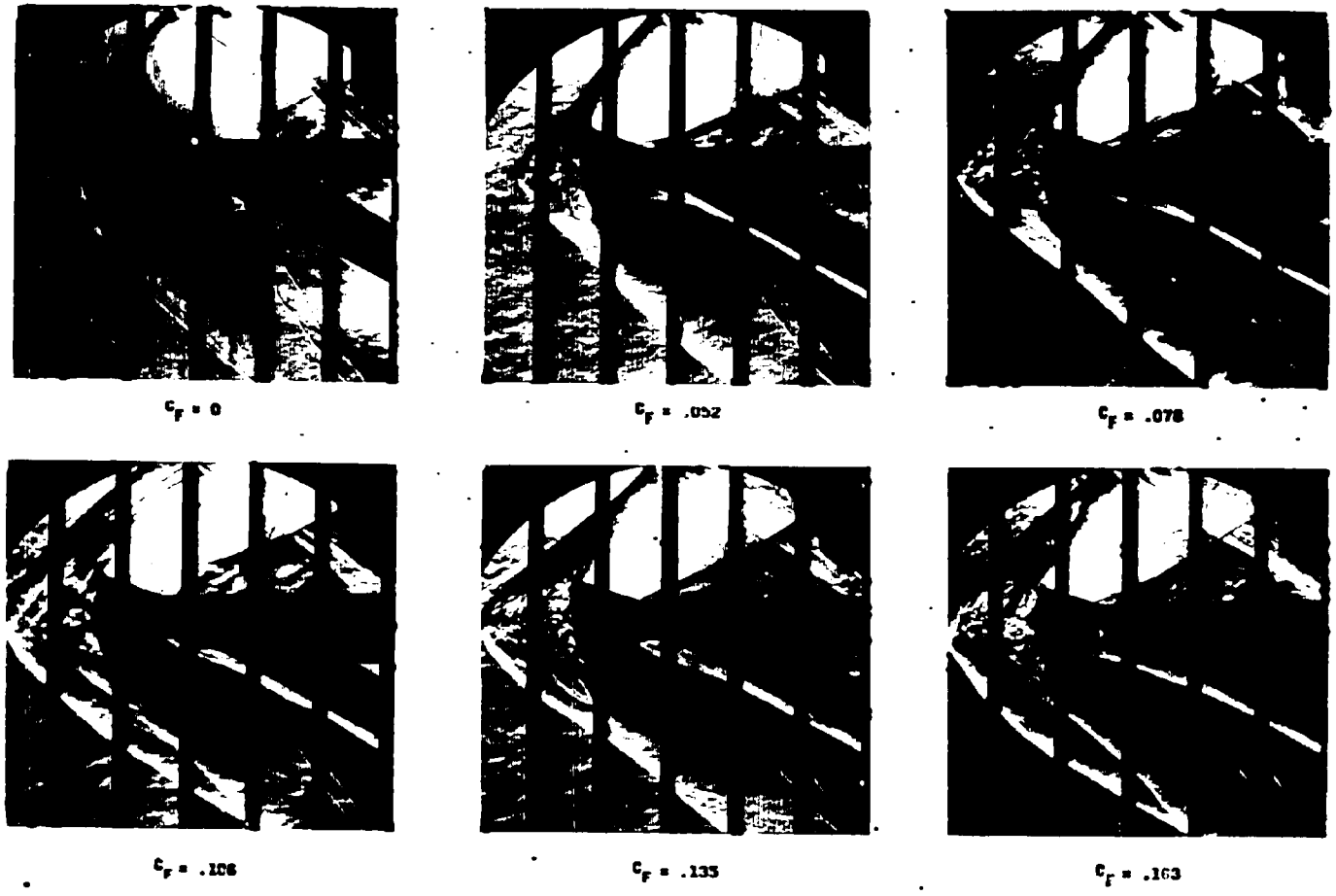

(b) M = 2.00.

L-61-1089

Figure 7.- Continued.

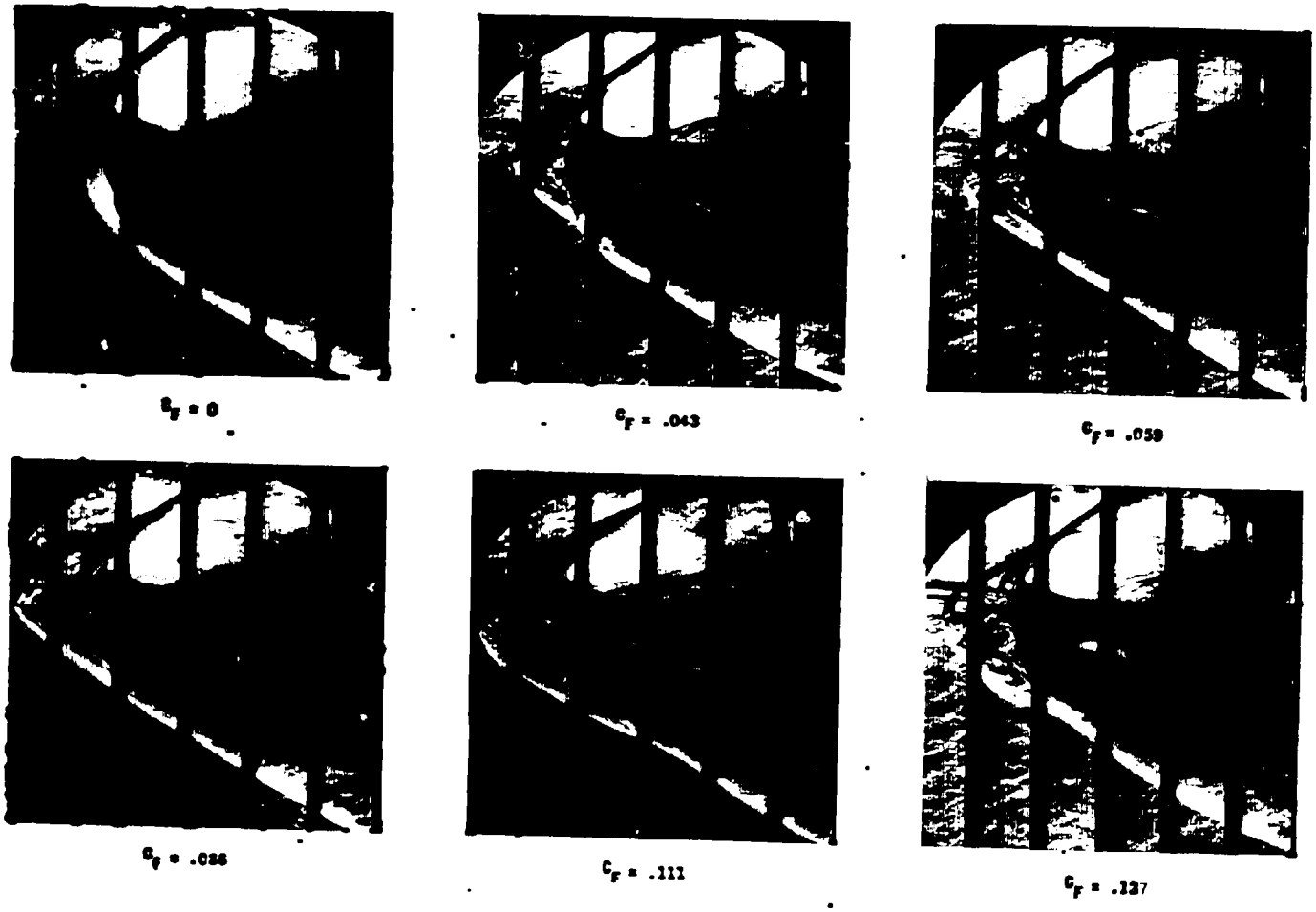

(c) M = 2.85.

L-61-1090

Figure 7.- Concluded.

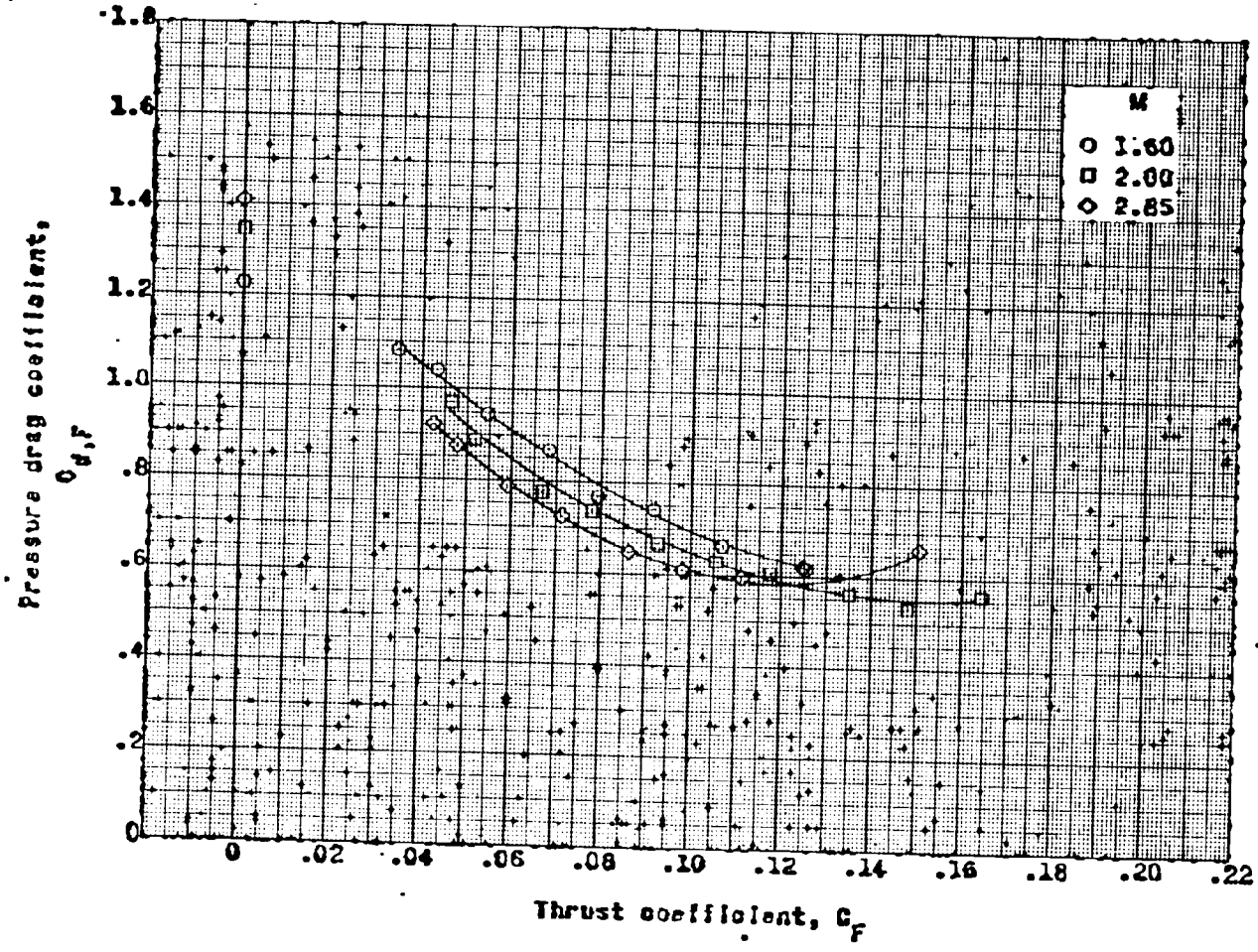

(a) Forebody.

Figure 8.- Pressure drag variation with thrust coefficient.

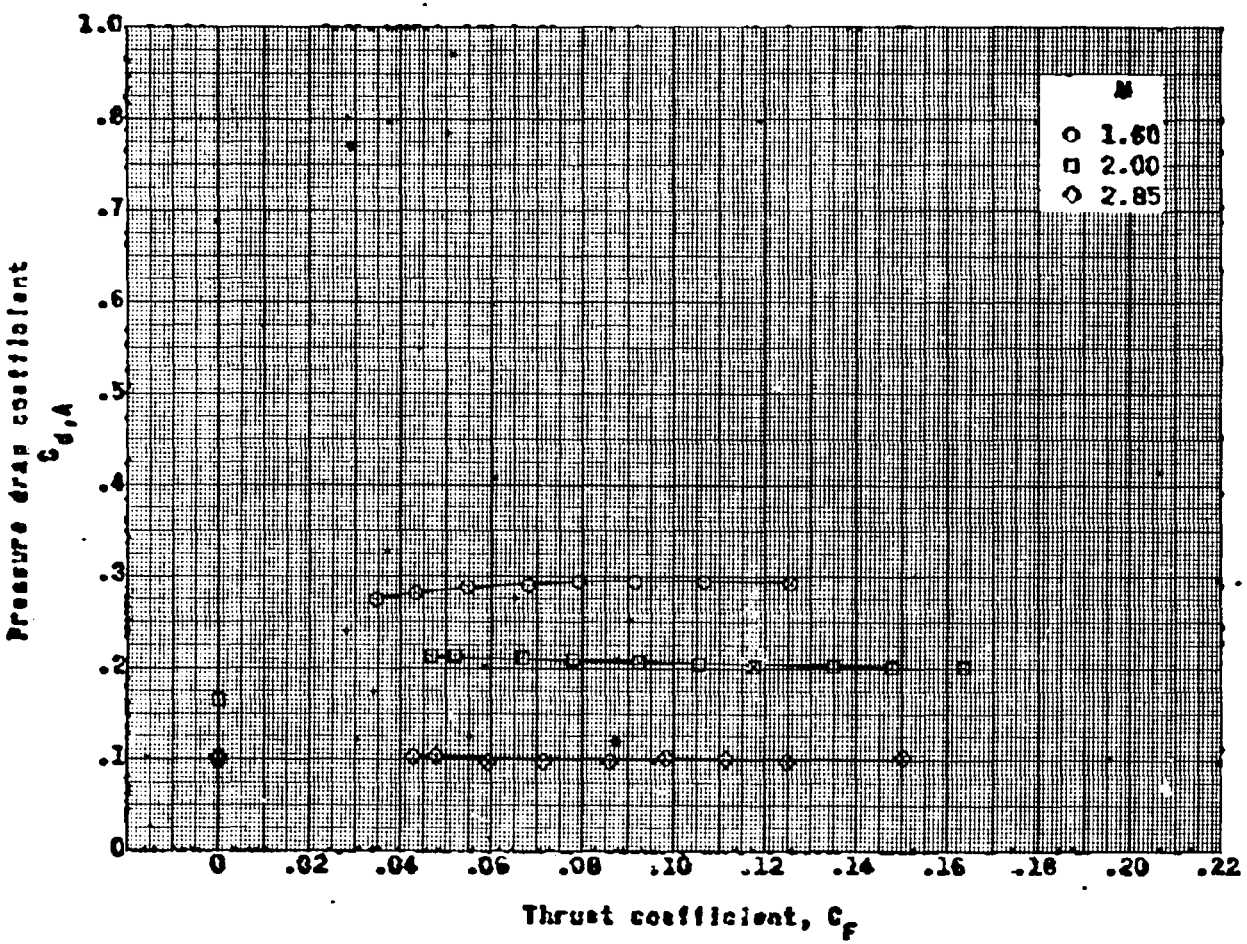

(b) Afterbody.

Figure 8.- Concluded.

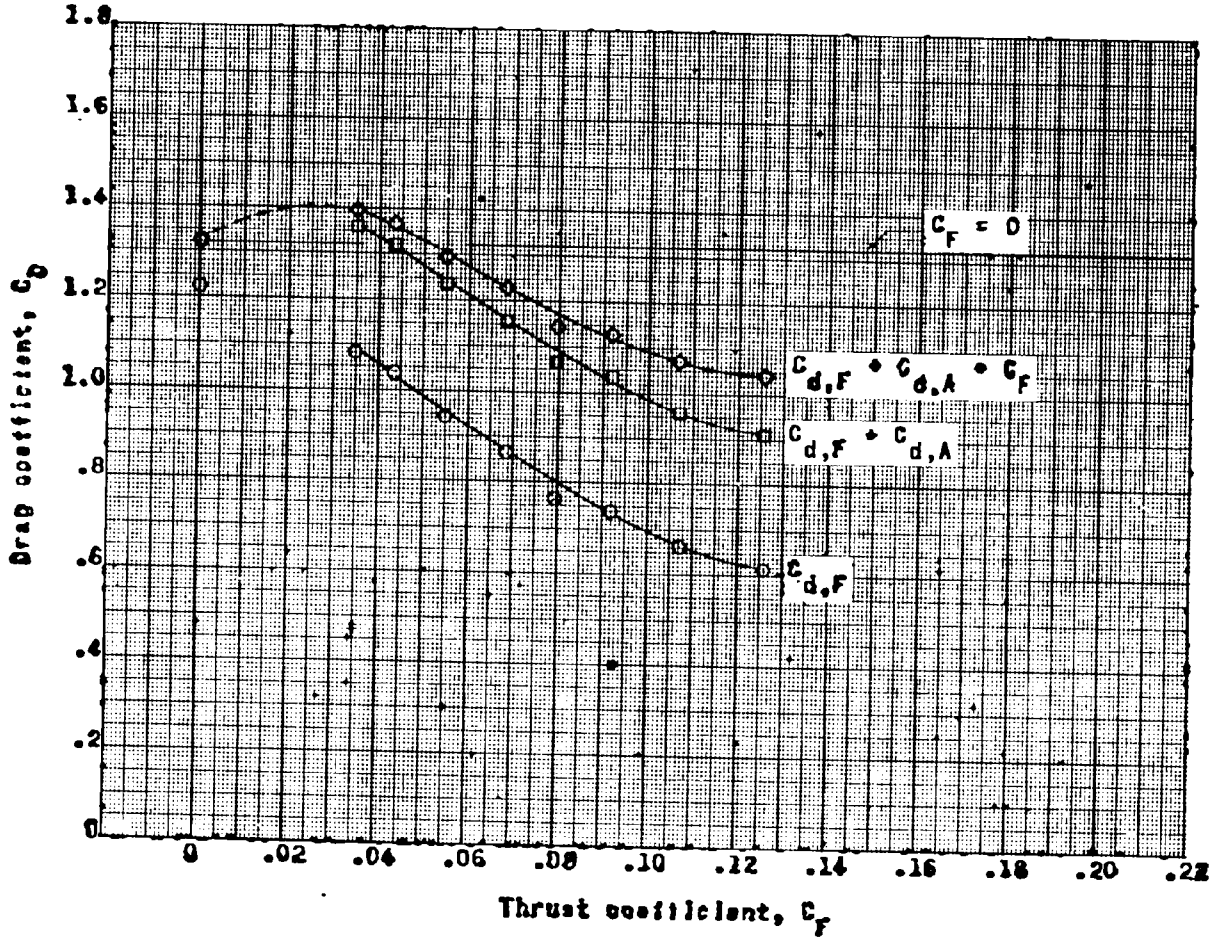

(a) M = 1.60.

Figure 9.- Drag variation with thrust coefficient.

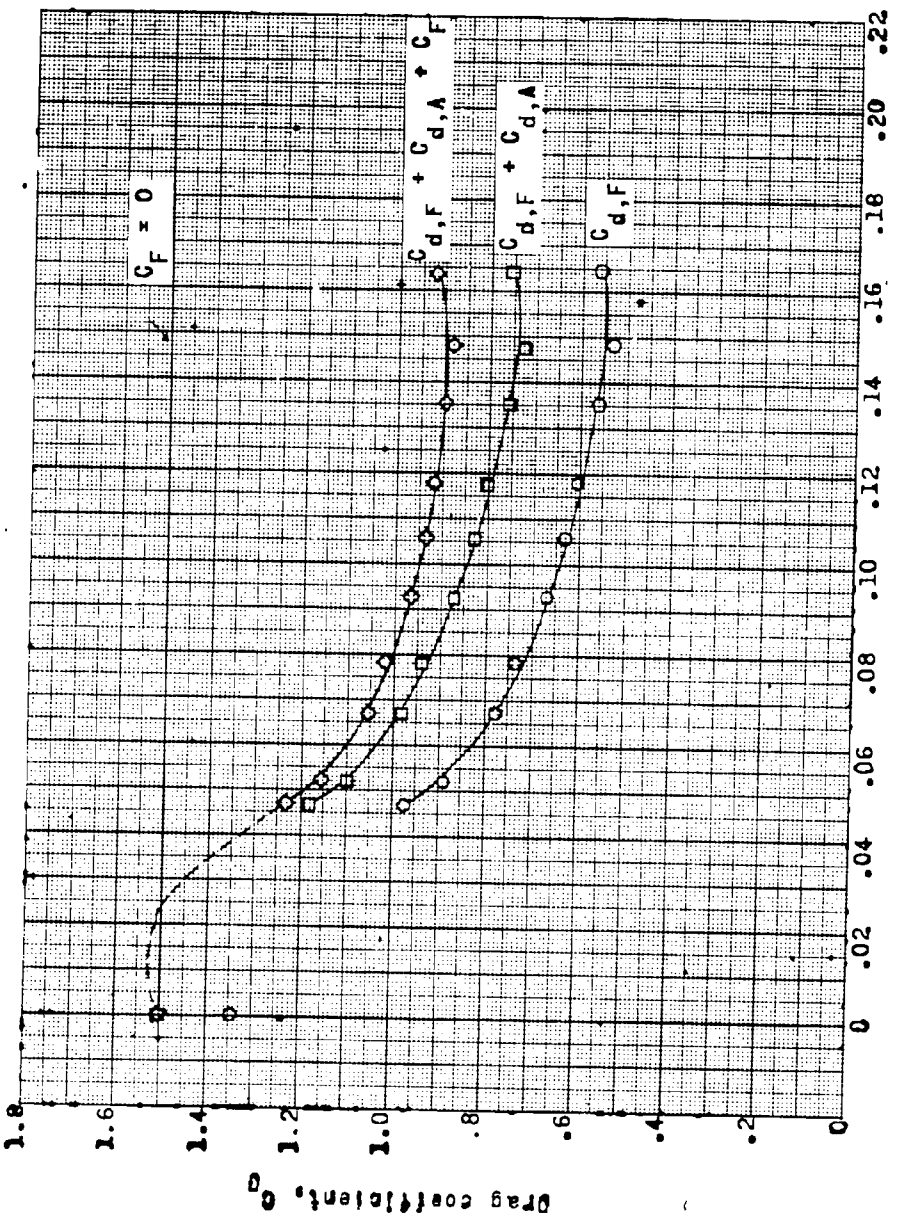

(b) M = 2.00.

Figure 9.- Continued.

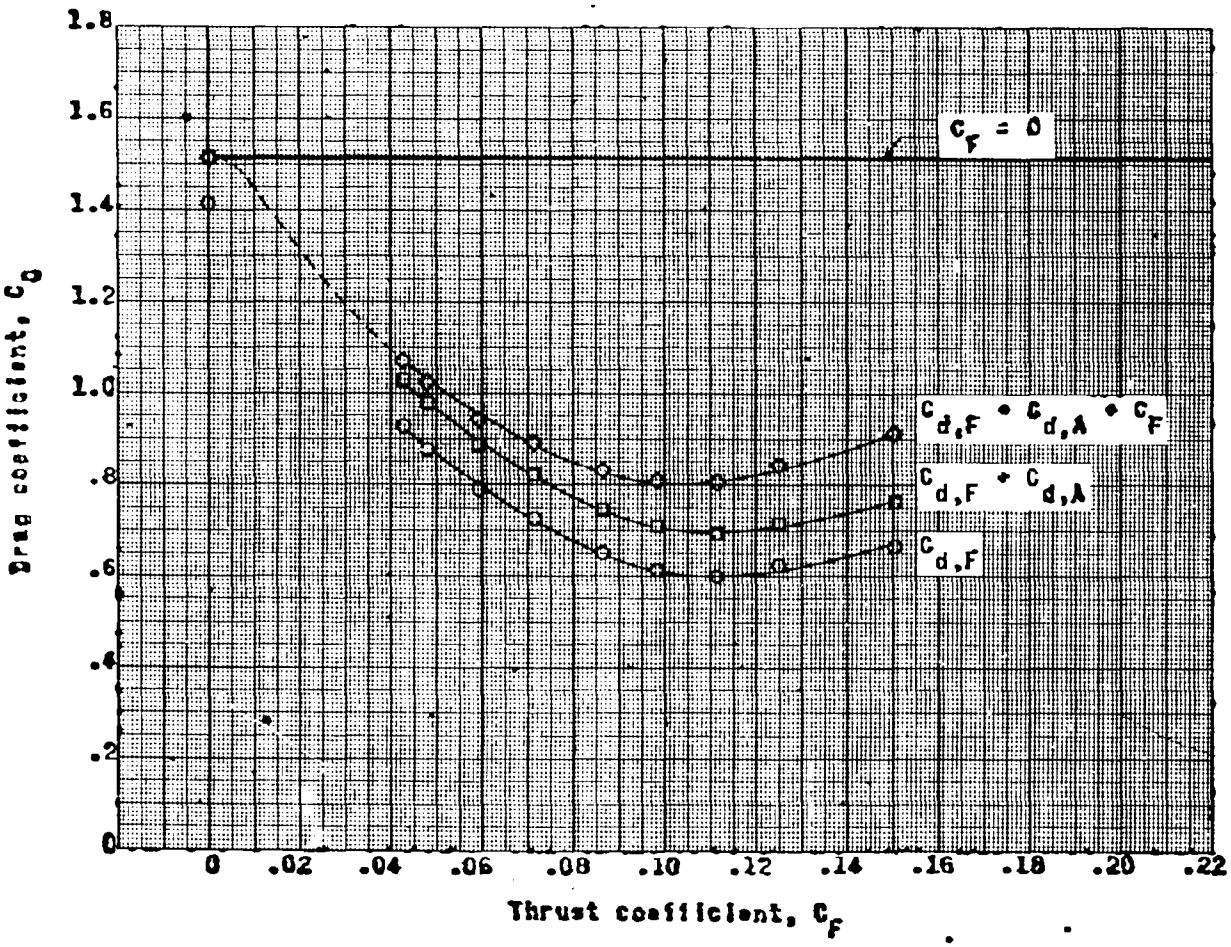

(c) $M = 2.85$.

Figure 9.- Concluded.

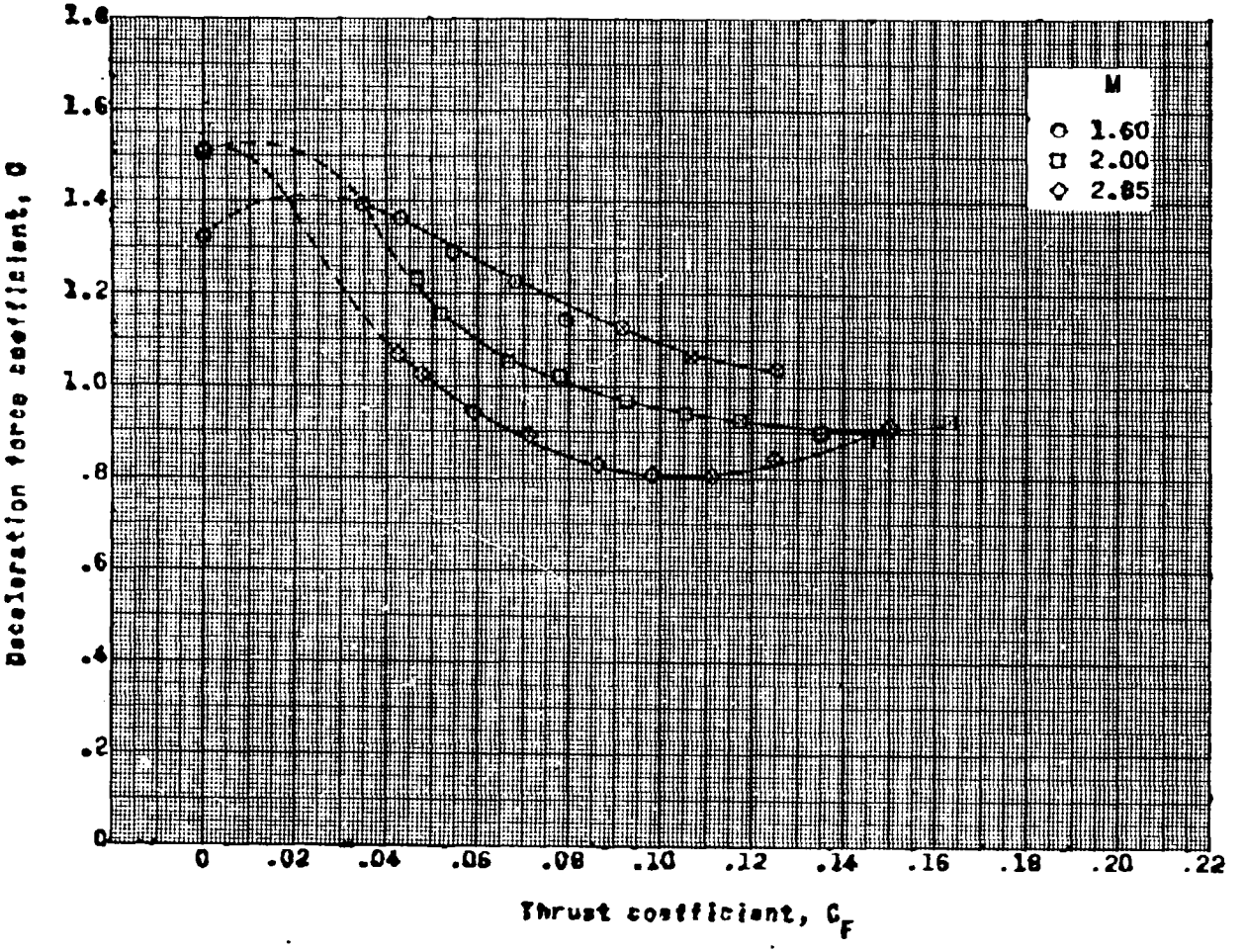

Figure 10.- Variation of total drag with the thrust coefficient at Mach numbers 1.60, 2.00, and 2.85.

NASA-Langley, 1961 L-1504

L-1504

NASA TN D-751
National Aeronautics and Space Administration.
INVESTIGATION OF A RETROROCKET EXHAUSTING FROM THE NOSE OF A BLUNT BODY INTO A SUPERSONIC FREE STREAM. Nickolai Charczenko and Katherine W. Hennessey. September 1961. 30p. OTS price, $0.75. (NASA TECHNICAL NOTE D-751)

The pressure distribution and pressure drag were determined on a blunt body which had a jet issuing from the nose at several free-stream Mach numbers. As a result of the retro-rocket operation a large decrease in pressure drag occurred at all Mach numbers investigated. At the same time, the retro-rocket caused very unstable flow about the model.

Copies obtainable from NASA, Washington

I. Charczenko, Nickolai
II. Hennessey, Katherine W.
III. NASA TN D-751

(Initial NASA distribution: 2, Aerodynamics, missiles and space vehicles; 5, Atmospheric entry.)

NASA

NASA TN D-751
National Aeronautics and Space Administration.
INVESTIGATION OF A RETROROCKET EXHAUSTING FROM THE NOSE OF A BLUNT BODY INTO A SUPERSONIC FREE STREAM. Nickolai Charczenko and Katherine W. Hennessey. September 1961. 30p. OTS price, $0.75. (NASA TECHNICAL NOTE D-751)

The pressure distribution and pressure drag were determined on a blunt body which had a jet issuing from the nose at several free-stream Mach numbers. As a result of the retro-rocket operation a large decrease in pressure drag occurred at all Mach numbers investigated. At the same time, the retro-rocket caused very unstable flow about the model.

Copies obtainable from NASA, Washington

I. Charczenko, Nickolai
II. Hennessey, Katherine W.
III. NASA TN D-751

(Initial NASA distribution: 2, Aerodynamics, missiles and space vehicles; 5, Atmospheric entry.)

NASA

NASA TN D-751
National Aeronautics and Space Administration.
INVESTIGATION OF A RETROROCKET EXHAUSTING FROM THE NOSE OF A BLUNT BODY INTO A SUPERSONIC FREE STREAM. Nickolai Charczenko and Katherine W. Hennessey. September 1961. 30p. OTS price, $0.75. (NASA TECHNICAL NOTE D-751)

The pressure distribution and pressure drag were determined on a blunt body which had a jet issuing from the nose at several free-stream Mach numbers. As a result of the retro-rocket operation a large decrease in pressure drag occurred at all Mach numbers investigated. At the same time, the retro-rocket caused very unstable flow about the model.

Copies obtainable from NASA, Washington

I. Charczenko, Nickolai
II. Hennessey, Katherine W.
III. NASA TN D-751

(Initial NASA distribution: 2, Aerodynamics, missiles and space vehicles; 5, Atmospheric entry.)

NASA

NASA TN D-751
National Aeronautics and Space Administration.
INVESTIGATION OF A RETROROCKET EXHAUSTING FROM THE NOSE OF A BLUNT BODY INTO A SUPERSONIC FREE STREAM. Nickolai Charczenko and Katherine W. Hennessey. September 1961. 30p. OTS price, $0.75. (NASA TECHNICAL NOTE D-751)

The pressure distribution and pressure drag were determined on a blunt body which had a jet issuing from the nose at several free-stream Mach numbers. As a result of the retro-rocket operation a large decrease in pressure drag occurred at all Mach numbers investigated. At the same time, the retro-rocket caused very unstable flow about the model.

Copies obtainable from NASA, Washington

I. Charczenko, Nickolai
II. Hennessey, Katherine W.
III. NASA TN D-751

(Initial NASA distribution: 2, Aerodynamics, missiles and space vehicles; 5, Atmospheric entry.)

NASA